(17) (a) B. K. Teo, P. A. Lee, A. L. Simons, P. Eisenberger, and B. M. Kincaid, *J. Am. Chem. Soc.*, **99**, 3854 (1977); (b) P. A. Lee, B. K. Teo, and A. L. Simons, *ibid.*, **99**, 3856 (1977).
(18) B. K. Teo, P. Eisenberger, and B. M. Kincaid, *J. Am. Chem. Soc.*, **100**, 1735 (1978).
(19) (a) B. K. Teo, K. Kijima, and R. Bau, *J. Am. Chem. Soc.*, **100**, 621 (1978); (b) B. K. Teo, P. Eisenberger, J. Reed, J. K. Barton, and S. J. Lippard, *ibid.*, **100**, 3225 (1978).
(20) (a) J. Reed, P. Eisenberger, B. K. Teo, and B. M. Kincaid, *J. Am. Chem. Soc.*, **99**, 5217 (1977); (b) J. Reed, P. Eisenberger, B. K. Teo, and B. M. Kincaid, *ibid.*, **100**, 2375 (1978).
(21) (a) S. P. Cramer, T. K. Eccles, F. Kutzler, K. O. Hodgson, and S. Doniach, *J. Am. Chem. Soc.*, **98**, 8059 (1976); (b) S. P. Cramer and K. O. Hodgson, *ibid.*, **100**, 2748 (1978).
(22) For example, if one arbitrarily defines ϕ_a of atom A (absorber), one can deduce ϕ_b of atom B (scatterer) from the experimental phase shift ϕ_{ab} for the atomic pair A–B. From ϕ_b one can then determine the central atom phase $\phi_{a'}$ of any atom A′ by measuring $\phi_{a'b}$ which is the total phase shift of atom pair A′B where A′ and B denote the (new) absorber and the (old) scatterer, respectively. Similarly, from ϕ_a it is possible to deduce the scatterer phase $\phi_{b'}$ of any atom B′ by measuring $\phi_{ab'}$ for the atom pair AB′ with A and B′ being the (old) absorber and the (new) scatterer, respectively. All individual phase functions constructed in this manner are "relative" to the arbitrarily defined ϕ_a of absorber A.
(23) S. M. Heald and E. A. Stern, *Phys. Rev. B*, **16**, 5549 (1977).
(24) In the matrix element the initial state should be that of a neutral atom and the final state that of an ion with a 2p hole. In our calculation, it is more convenient to use either the neutral atom or the ion wave functions for both the initial and final states. The ratios M_{21}/M_{01} obtained using these two methods are found to be in agreement to within a few percent even though the individual matrix elements show bigger variation. The result using the ion wave functions has been plotted in Figure 1. We should also mention that there is a considerable amount of literature dealing with M_{21}/M_{01} for light elements or outer shells. See, for instance, O. J. Kennedy and S. T. Manson, *Phys. Rev. A*, **5**, 227 (1972); K. Codling, R. G. Houlgate, J. B. West, and P. R. Woodruff, *J. Phys. B*, **9**, L83 (1976).
(25) F. W. Lytle, D. E. Sayers, and E. A. Stern, *Phys. Rev. B*, **15**, 2426 (1977).
(26) (a) E. Clementi and C. Roetti, *At. Data Nucl. Data Tables*, **14**, 177 (1974); (b) F. Herman and S. Skillman, "Atomic Structure Calculations", Prentice-Hall, Englewood Cliffs, N.J., 1963.
(27) N. F. Mott, *Proc. R. Soc. London, Ser. A*, **124**, 425 (1925); **135**, 429 (1932); M. Fink and A. C. Yates, *At. Data*, **1**, 385 (1970).
(28) The theoretical amplitude functions, which include inelastic processes in the scattering atom, are found to be off by ~50%. Part of this discrepancy is due to core relaxation effects. Furthermore, the amplitude is expected to be somewhat sensitive to the chemical environment and will depend on the distance r_i (due to an exponential damping factor $e^{-2r_i/\lambda}$). An overall scale factor is therefore included in the refinements.
(29) "International Tables for X-ray Crystallography", Vol. III, Kynoch Press, Birmingham, England, 1968, pp 161, 172.
(30) L. Pauling, "The Nature of the Chemical Bond", 3rd ed., Cornell University Press, Ithaca, N.Y., 1960, p 403.
(31) P. Rabe, G. Tolkiehn, and A. Werner, *J. Phys. C*, in press.

Resonance Raman Spectroelectrochemistry. 6. Ultraviolet Laser Excitation of the Tetracyanoquinodimethane Dianion

Richard P. Van Duyne,*[1a,b] Mary R. Suchanski,[1c] Joseph M. Lakovits,[1a] Allen R. Siedle,[1d] Keith D. Parks,[1a] and Therese M. Cotton[1a,e]

Contribution from the Department of Chemistry, Northwestern University, Evanston, Illinois 60201, and the Central Research Laboratories, 3M Company, St. Paul, Minnesota 55101. *Received November 27, 1978*

Abstract: The resonance Raman spectrum has been obtained for the electrogenerated dianion of tetracyanoquinodimethane (TCNQ) upon excitation of its lowest energy electronic transition (λ_{max} 330 nm) with a frequency doubled, flashlamp-pumped, Rhodamine 640 dye laser. For comparison we report the normal Raman spectrum of solid $Li_2TCNQ\cdot THF$. The electron transfer induced frequency shifts for the second reduction step of TCNQ are measured and interpreted using the π-bond order changes determined from SCF-MO-CI and INDO/S electronic structure calculations as well as the π-bond length changes determined from a MNDO-SCF-MO calculation. Finally, the $TCNQ^{2-}$ Raman data is used to identify the oxidation state of TCNQ in the coordination complex $[Co(acacen)(py)_2]_2TCNQ$.

Introduction

It is now widely recognized that the observables in resonance Raman spectroscopy (RRS) (viz., vibrational frequency, resonance-enhanced vibrational symmetry type, number and intensity pattern of overtones, and depolarization ratios) and their laser excitation wavelength dependence represent sensitive probes of the molecular and electronic structure changes that can occur in molecules. Such structure changes are commonly induced by chemical modification, electron-transfer (ET) reactions, and optical excitation. Our primary motivation for applying RRS to the study of molecular and electronic structure changes stems from a long-term interest in developing a detailed description of ET processes. In particular we have been concerned with evaluating the role of intramolecular vibrational energy dissipation processes in highly exothermic, homogeneous, ET reactions.[2-7] To compare such ET theories with experiment, information is needed concerning the magnitude of the specific structural changes (viz., bond length, vibrational frequency, and anharmonicity) which occur within the donor and acceptor molecules during an ET process. In addition we are interested in studying the molecular and/or electronic structure changes that accompany the partial ET reactions involved in the formation of donor-acceptor, charge-transfer complexes that behave as one-dimensional, organic, electrical conductors.[8-12,41] Thus the technique of resonance Raman spectroelectrochemistry (RRSE) was developed[13] as a convenient means of coupling the observational sensitivity of RRS for monitoring molecular and electronic structure changes with the ability of electrochemistry to initiate and cleanly carry out successive one-electron transfer reactions.

Tetracyanoquinodimethane (TCNQ) was chosen for study by RRSE because it is a strong electron-acceptor molecule,[8] is the acceptor half of the prototype one-dimensional, organic metal tetrathiafulvalene-tetracyanoquinodimethane[8,9] (TTF-TCNQ) and exhibits two successive, one-electron reductions that are both chemically and electrochemically reversible in deoxygenated, aprotic solvents:[14]

$$TCNQ^0\,(^1A_g) + e^- \rightleftharpoons TCNQ^{-}\cdot(^2B_{3g}) \quad (1)$$

$$TCNQ^{-}\cdot(^2B_{3g}) + e^- \rightleftharpoons TCNQ^{2-}(^1A_g) \quad (2)$$

RRSE with visible ion laser lines has been used to obtain the RRS of the $^2B_{3g}$ (viz., D_{2h} point group) ground state of the

0002-7863/79/1501-2832$01.00/0

TCNQ radical anion.[14] The vibrational frequency shifts associated with the first reduction step (eq 1) for most of the totally symmetric normal modes of TCNQ have been obtained by comparing the RRS of $TCNQ^{-}\cdot$ with the pre-RRS of $TCNQ^{0}$. The ν_2 C≡N stretch, the ν_4 exocyclic C=C stretch, and the ν_6 C—C ring stretch showed the largest $1e^-$ transfer induced frequency shifts (viz., $\Delta\nu_2 = -31$ cm^{-1}, $\Delta\nu_4 = -64$ cm^{-1}, and $\Delta\nu_6 = +28$ cm^{-1}).[15]

In order to measure the vibrational frequency shifts and other vibrational properties associated with the second one-electron reduction step of TCNQ (eq 2), we require the RRS of $TCNQ^{2-}$ (^1A_g). Although we were initially led to believe that this spectrum could be obtained with visible laser excitation frequencies,[16] further study showed that $TCNQ^{2-}$ absorbs only in the ultraviolet with maxima at 330, 240, and 210 nm.[17] Continuing advances in laser technology, particularly in tunable dye lasers, have provided new opportunities for the chemist to exploit the RR phenomenon. Ultraviolet RRS is now practical using the discrete UV frequencies available from Ar^+, Kr^+, and He-Cd lasers,[18-25] the second harmonics of ion laser lines,[12,18] and the tunable UV radiation available from frequency doubled, pulsed dye lasers.[26-28]

This paper reports the ultraviolet RRS of electrogenerated $TCNQ^{2-}$ (^1A_g) using a frequency doubled, flashlamp-pumped, dye laser as the excitation source. The RRS of $TCNQ^{2-}$ in solution is compared with the CW Ar^+ laser excited NRS of solid dilithium tetracyanoquinodimethandiide tetrahydrofuranate ($Li_2TCNQ\cdot THF$). The vibrational frequency shifts accompanying the second reduction step of TCNQ are reported and analyzed by comparison with the π-bond order changes and bond-length changes obtained from various electronic structure calculations on $TCNQ^{-}\cdot(^2B_{3g})$ and $TCNQ^{2-}$ (^1A_g). Finally the utility of this new Raman data on $TCNQ^{2-}$ as an aid in the identification of the TCNQ oxidation state in a Co(II) coordination complex will be demonstrated.

Experimental Section

Materials. The sources of and purification methods for TCNQ have been previously described.[14] Solutions of TCNQ (ca. 5×10^{-4} M) in acetonitrile with tetrabutylammonium perchlorate (TBAP, ca. 0.1 M) as the supporting electrolyte were thoroughly degassed by repeated freeze-pump-thaw (F-P-T) cycles under diffusion pump vacuum and stored under high-purity nitrogen. $TCNQ^{2-}$ (^1A_g) was electrochemically prepared by controlled-potential electrolysis in a vacuum tight cell (see Figure 1) at −0.95 V vs. a platinum quasi-reference electrode (PtQRE). Both coulometry and UV-vis absorption spectroscopy showed that the two-electron reduction under these conditions is complete (i.e., $n_{app} = 2.00 \pm 0.02$; λ_{max} ($TCNQ^{2-}$) 330 nm, ϵ 3.1×10^4 M^{-1} cm^{-1}), and reversible (i.e., $Q_b/Q_f = 0.99 \pm 0.02$; λ_{max} ($TCNQ^0$) 390 nm, ϵ 7.0×10^4 M^{-1} cm^{-1}). The total duration of the reversal coulometry experiment was 4×10^3 s so that the Q_b/Q_f ratio of ca. 1 indicates the chemical stability of $TCNQ^{2-}$ for at least this length of time.

Dilithium tetracyanoquinodimethandiide tetrahydrofuranate ($Li_2TCNQ\cdot THF$) (**1**) was prepared in 90% yield by the addition of 2 equiv of *n*-butyllithium to 1,4-bis(dicyanomethyl)benzene in tetrahydrofuran. The white precipitate was isolated by Schlenk filtration and drying under high vacuum. Anal. Calcd for $C_{16}H_{14}Li_2N_4O$: H, 4.14. Found: C, 66.25; N, 19.31; H, 4.43. Either in solution or in the solid state, **1** was extremely sensitive to oxygen and moisture, turning red after brief exposure to air.

Oxidation of **1** in tetrahydrofuran with excess tetracyanoethylene produced purple $LiTCNQ$[29] in 81% yield. Alkylation was achieved by stirring a benzene suspension of **1** with methyl fluorosulfonate to form 1,4-bis(1,1-dicyanoethyl)benzene (**2**), in 27% yield: mp 185 °C; $\delta_{acetone}$ −7.95 (s, 2 H) and −2.30 (s, 3 H) ppm; IR (KBr) 2250 (ν_{CN}) and 835 cm^{-1}. Anal. Calcd for $C_{14}H_{10}N_4$: H, 4.27. Found: C, 71.52; H, 4.19. Electron impact fragmentation of **2** occurred by loss of methyl groups and the mass spectrum showed peaks at *m/e* 234 (M^+, 20), 219 [$(M - CH_3)^+$, 100], and 204 [$(M - 2CH_3)^+$, 11]. The reaction of **1** with deuterium chloride in anhydrous tetrahydrofuran produced the deuterated derivative in 90% yield, $\delta_{acetone}$ −8.90 ppm, *m/e* 208.

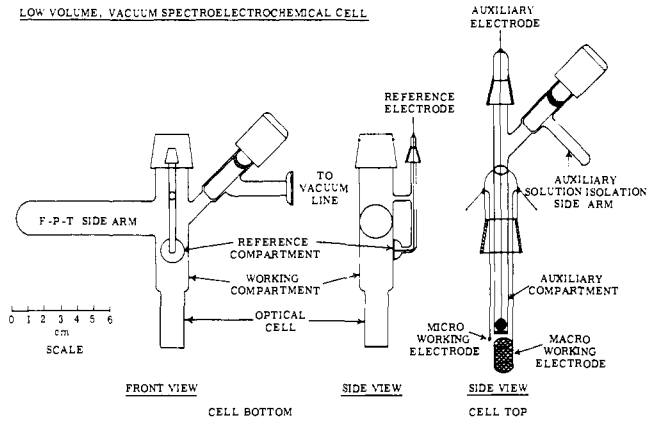

Figure 1. Low-volume, vacuum spectroelectrochemical cell.

The cobalt(II) Schiff's base chelate *N,N'*-ethylenebis(acetylacetoniminato)cobalt(II), Co(acacen), was prepared by the method of Carter.[30] Anal. Found for $C_{12}H_{18}CoN_2O_2$: C, 51.07; H, 6.45; N, 9.96. The 2:1 complex of this compound with TCNQ in the presence of pyridine (py), $[Co(acacen)(py)_2]_2TCNQ$ (**3**), was prepared according to method 2 of Basolo et al.[31] Anal. Calcd for $C_{56}H_{60}Co_2N_{12}O_4$: H, 5.54; N, 15.52. Found: C, 62.20; H, 5.89; N, 15.29.

Apparatus. The general experimental arrangement for carrying out RRSE experiments in bulk solution using controlled-potential electrolysis (coulometry) as the electrogeneration mode has been previously described.[13,14,32] The great reactivity of $TCNQ^{2-}$ toward atmospheric oxygen combined with its UV absorption properties[17] has, however, necessitated some modifications of the previously described electrochemical cells, laser excitation sources, and photon detection electronics.

A low-volume (viz., ca. 5-10 mL), vacuum tight (viz., ca. 10^{-5} Torr) spectroelectrochemical cell was designed specifically for the RRSE studies of $TCNQ^{2-}$ as well as for the radical ions involved in photosynthesis.[33,34] This one cell, shown in detail in Figure 1, provides the capability for carrying out the following experiments on the same electroactive sample: (1) cyclic voltammetry; (2) double potential step chronoamperometry and chronocoulometry; (3) cyclic differential pulse voltammetry;[35] (4) UV-vis electronic absorption spectroscopy in either a 1.0-cm or a 1.0-mm (viz., a 9.0-mm quartz spacer can be inserted in the normally 1.0-cm cell) path length cell; (5) RRS in either the F-P-T side arm or in the spectrophotometric cell. All of the electroanalytical experiments employing the micro-working electrode as well as the spectroanalytical experiments can be carried out before and after bulk electrolysis at the macro-working electrode. The vacuum spectroelectrochemical cell is first charged with solids in a drybox (viz., the electroactive compound and the supporting electrolyte), attached to a vacuum line, and pumped down to 10^{-5} Torr to dry these materials. Bulb-to-bulb transfer of previously dried and degassed nonaqueous solvent completes the cell loading operation. Since these various manipulations may require tipping the loaded cell on its side, an evacuated auxiliary solution side arm is provided to trap the auxiliary electrode compartment solution, which may contain fluorescent materials, so that it will not contaminate the solution in the working electrode compartment. All-quartz construction provides UV transparency.

The laser excitation source for these experiments is a pulsed, flashlamp-pumped, tunable dye laser fitted with intracavity frequency doubling crystals (Chromatix, CMX-4) for UV generation rather than the CW argon ion laser pumped dye lasers used previously. The pulsed dye laser was operated with Rhodamine 640 dye (Exciton) which produced ca. 2.5 mW average power at 330 nm and 10 Hz repetition rate. A 1.0-m, holographic grating, double monochromator (Jobin-Yvon Ramanor HG-2) was used in second order in conjunction with a cooled (−20 °C), high quantum efficiency photomultiplier tube (PMT = RCA C31034) to detect the UV RR scattered photons from the $TCNQ^{2-}$ sample.

The photon detection electronics and signal processing system consists of a gain = 200 pulse amplifier (Ortec Model 9301/9302)

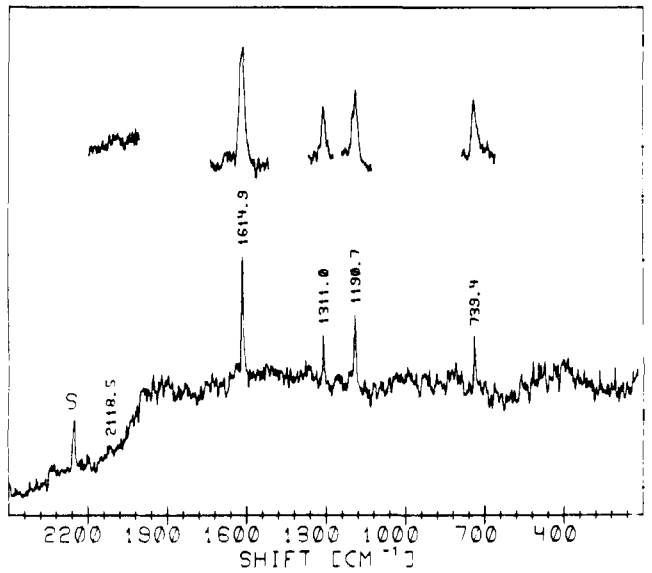

Figure 2. Resonance Raman spectrum of electrogenerated $TCNQ^{2-}$ (5×10^{-4} M) in acetonitrile with 0.1 M tetrabutylammonium perchlorate as supporting electrolyte. Average laser power at 329.8 nm = 2.5 mW at 10 Hz repetition rate; band-pass = 4.0 cm^{-1}; scan rate = 50 cm^{-1} min^{-1}; counting gate = 1.00 s; arbitrary intensity units. Bottom: composite plot of the spectrum from 100 to 2500 cm^{-1} at 300 cm^{-1}/in. with smoothing. Top: expanded scale plot of Raman bands at 125 cm^{-1}/in. without smoothing.

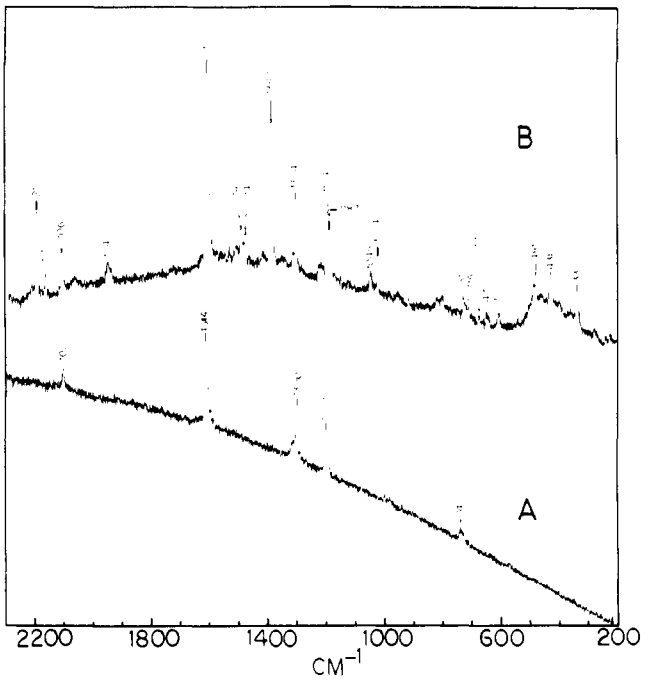

Figure 3. Normal Raman spectra of (A) $Li_2TCNQ{\cdot}THF$, laser power at 457.9 nm = 10 mW, band-pass = 2.0 cm^{-1}. (B) $(Co(acacen)(py)_2)_2$-TCNQ, laser power at 647.1 nm = 20 mW, band-pass = 4.0 cm^{-1}. Both samples were solid powders. Spectra were scanned at ca. 50 cm^{-1} min^{-1} using a 1.00-s counting gate. Plasma lines were removed at 457.9 nm with an interference filter and at 647.1 nm with a Claassen filter.

connected to the PMT which produces a current pulse that is identical in shape with the laser excitation pulse (viz., approximately Gaussian with fwhm = 1 μs). This current pulse, representing the UV RR signal, is integrated over a 10-μs gating interval in the signal channel of a dual-channel, gated integrator. This gate interval was selected as a compromise between minimizing uncorrelated system noise and clipping the RR signal due to pulse-to-pulse laser triggering jitter. The reference channel of the gated integrator was used to monitor the laser pulse energy with a UV filtered photomultiplier tube (RCA 1P 28). The output signals from the signal and reference channels of the gated integrator were ratioed and averaged using an analog multiplier unit (Princeton Applied Research Model 230). The output of the multiplier was converted to a TTL pulse train with a voltage-to-frequency converter and recorded by standard TTL pulse counting electronics. The entire UV RRSE experiment is controlled by a Nova 2/10 minicomputer equipped with 65K bytes of memory, dual floppy disks, a CRT terminal, a line printer, and an incremental plotter.

Methods. Both RR and NR spectra are excited using backscattering geometry with S1-UV grade quartz collection and focusing optics. The laser light is focused to a slit-shaped image on the cell, the Raman scattered light is collected and focused, and then the image on the cell, is rotated 90° with a dove prism to match the horizontal slits of the double monochromator. The Raman spectra obtained on solid powder samples (viz., compounds **1** and **3**) employed the CW Raman instrumentation described previously.[13,14,32] Solid samples were spun and liquid samples stirred to provide relative motion between the laser beam and the sample focal spot so that laser-induced thermal decomposition could be minimized.

Results and Discussion

RRSE of $TCNQ^{2-}$ and NRS of $Li_2TCNQ{\cdot}THF$. The UV excited RRS of electrochemically generated $TCNQ^{2-}$ is presented in Figure 2. This spectrum was recorded in segments, combined, and smoothed using the computer algorithm based on the simplified least-squares method of Savitsky and Golay.[36] Four of the totally symmetric fundamentals of $TCNQ^{2-}$ are clearly seen in this spectrum and are assigned by analogy with the previous results on $TCNQ^0$ and $TCNQ^{-}{\cdot}(^2B_{3g})$[14] as ν_3 1615 cm^{-1} (predominantly C=C and C—C ring stretching but this normal mode also contains some exocyclic C=C stretching and some C—H bending character), ν_4 1311 cm^{-1} (ring C=C stretch + exocyclic C=C stretch), ν_5 1191 cm^{-1} (C—H bend), and ν_7 739 cm^{-1} (ring C—C stretch + exocyclic C—C stretch). A possible fifth totally symmetric mode is observed with very low S/N and could be assigned as ν_2 2119 cm^{-1} (C≡N stretch). The absence of the other five totally symmetric modes (viz., ν_1 C—H stretch, ν_6 ring C—C stretch + exocyclic C—C stretch, ν_8 exocyclic C—C stretch + C—C≡N bend + C—C—C bend, ν_9 C—C—C ring bend + C—C≡N bend, and ν_{10} C—C≡N bend + C—C—C bend) from the $TCNQ^{2-}$ RR spectrum shown in Figure 2 indicates that the bond-length changes corresponding to these normal modes undergo only very small displacements when $TCNQ^{2-}$ is excited in the region of its lowest electronic transition with the UV laser. The intensity of RR lines is directly proportional to the bond-length changes that accompany excitation of a molecule into an excited state. When these bond-length changes are small, the exciting laser power is low, and the background signal is relatively high, as is the case in these $TCNQ^{2-}$ RRS experiments, it is very difficult to observe such lines.

Supporting evidence for the validity of the $TCNQ^{2-}$ RR spectrum and the proposed assignment comes from the CW argon ion laser excited (viz., 457.9 nm) NR spectrum of $Li_2TCNQ{\cdot}THF$ (**1**). This spectrum is shown in Figure 3A. Five totally symmetric fundamentals are clearly observed and assigned as ν_2 2102 cm^{-1}; ν_3 1614 cm^{-1}, ν_4 1300 cm^{-1}, ν_5 1200 cm^{-1}, ν_7 740 cm^{-1}. No bands in the NRS of **1** correspond to the known vibrations of tetrahydrofuran.[37,38] The assertion that compound **1** is, in fact, a solid-state $TCNQ^{2-}$ containing species is further supported by infrared and ^1H NMR data. The IR spectrum of **1** in a Nujol mull contained absorptions at 2180 (s) and 2105 cm^{-1} (s) that can be assigned as ν_{CN}. In addition there are other absorptions at 1375, 1040 (m), and 820 cm^{-1} (m). The ^1H NMR spectrum of **1** in dimethyl-d_6 sulfoxide contained a singlet at δ 6.53 (1 H) and two complex multiplets centered at δ 3.62 and 1.75, 1 H each, due to the AB

Table I. Totally Symmetric Raman Fundamentals of $TCNQ^0$, $TCNQ^{-}\cdot$ and $TCNQ^{2-}$

mode ν_i	$TCNQ^0$ soln[a] 457.9 nm, cm^{-1}	$TCNQ^0$ solid[b] 457.9 nm, cm^{-1}	$TCNQ^{-}\cdot$ soln[a] 647.1 nm, cm^{-1}	$TCNQ^{-}\cdot$ solid[c] 457.9 nm, cm^{-1}	$TCNQ^{2-}$ soln 329.8 nm, cm^{-1}	$TCNQ^{2-}$ solid[d] 457.9 nm, cm^{-1}	ET shift $\Delta\nu_{i,1}$,[e] cm^{-1}	ET shift $\Delta\nu_{i,2}$,[e] cm^{-1}
ν_1		3048						
ν_2	2223	2229	2192	2218	2119	2102	−31	−73
ν_3	1603	1602	1613	1608	1615	1614	+10	+2
ν_4	1453	1454	1389	1379[f]	1311	1300	−64	−78
ν_5	1192	1207	1195	1207	1191	1200	+3	−4
ν_6	948	948	976	980			+28	
ν_7	707	711	724	729	739	740	+17	+15
ν_8	598	602	612	609			+14	
ν_9	331	334	336	341			+5	
ν_{10}		144						

[a] From ref 14. [b] From ref 39. [c] LiTCNQ; from ref 40. [d] $Li_2TCNQ\cdot THF$; this work. [e] Solution-phase frequency shifts according to the convention in note 15. [f] Split band in solid state; components are 1394 and 1379 cm^{-1}.

Table II. Bond-Order and Bond-Length Changes in TCNQ

K_i[a]	$\Delta p_{i,1}$[b]	$\Delta p_{i,2}$[b]	$\Delta p_{i,1}$[c]	$\Delta p_{i,2}$[c]	$\Delta r_{i,1}$,[d] pm	$\Delta r_{i,2}$,[d] pm
K_1	−0.09	−0.10	−0.105	−0.081	+2.0	+1.6
K_2	+0.13	+0.15	+0.140	+0.100	−2.8	−2.1
K_3	−0.20	−0.23	−0.212	−0.182	+3.9	+4.3
K_4	+0.09	+0.13	+0.065	+0.051	−1.7	−1.1
K_5	−0.05	−0.08	−0.031	−0.032	+0.1	+0.9

[a] Assignments from ref 39. [b] $\Delta p_{i,1} = p_i(TCNQ^{-}\cdot) - p_i(TCNQ^0)$; $\Delta p_{i,2} = p_i(TCNQ^{2-}) - p_i(TCNQ^{-}\cdot)$; p_i from ref 16. [c] From ref 42. [d] $\Delta r_{i,1} = r_i(TCNQ^{-}\cdot) - r_i(TCNQ^0)$; $\Delta r_{i,2} = r_i(TCNQ^{2-}) - r_i(TCNQ^{-}\cdot)$; r_i from ref 44.

spin pattern of the coordinated tetrahydrofuran. This data should be compared to the ^1H NMR spectrum of 1,4-bis(dicyanomethyl)benzene, the starting material, which exhibited singlets at $\delta_{acetone}$ 7.90 (2 H) and 6.20 (1 H). These IR and NMR data suggest that $TCNQ^{2-}$ is effectively a 1,4-disubstituted benzene containing two electropositive substituents.

Table I summarizes the totally symmetric vibrational data for $TCNQ^0$, $TCNQ^{-}\cdot$, and $TCNQ^{2-}$ in both the solid state and in solution. Also listed in Table I are the observed vibrational frequency shifts which accompany the successive one-electron transfer steps (i.e., reductions) for TCNQ in solution. It should be noted that the discrepancies between the observed frequencies for the totally symmetric modes of electrogenerated $TCNQ^{2-}$ and chemically generated solid-state $TCNQ^{2-}$ in the form of the dilithium salt, **1**, are small enough to be understood in terms of a lithium cation perturbation, such as that found in comparing electrogenerated $TCNQ^{-}\cdot$ and chemically formed LiTCNQ solid, rather than a fundamental structural difference. The data compiled in Table I clearly show that modes ν_2 and ν_4 are the most sensitive to changes in the electronic structure of the TCNQ moiety. These two modes are therefore expected to be highly selective vibrational diagnostics for determining the oxidation state of TCNQ in charge-transfer complexes[41] and coordination complexes (see below).

Analysis of the ET Induced Vibrational Frequency Shifts. In our earlier work on the first reduction step of TCNQ,[14] we developed an approximate method for the analysis of the ET induced frequency shifts. This method was based on the comparison of the observed frequency shift with a calculated, π-bond order change, $\Delta P_{i,total}$, for each of the i normal modes. The bond-order changes for each of the individual bond stretching internal coordinates, Δp_i, were obtained from electronic structure calculations on $TCNQ^0$ and $TCNQ^{-}\cdot$ based on the SCF-MO-CI[16] and INDO/S[42] procedures. The Δp_i were then weighted by the fractional contribution that a particular bond stretching coordinate, K_i, makes to the potential energy distribution (PED) for each totally symmetric normal mode. The PED used was that from the work of Girlando and Pecile[39] on the normal coordinate analysis (NCA) of $TCNQ^0$. Angle bending coordinates are assigned PED weighting factors of zero in computing the total PED weighted bond order change, $\Delta P_{i,total}$, for each normal mode from

$$\Delta P_{i,total} = \sum_i (PED)_{K_i} \Delta p_i \qquad (3)$$

We would now like to extend this analysis to the case of the second electron-transfer step in TCNQ (eq 2). An extension of our previous analysis is also possible since Pecile et al.[43] have published the PED for $TCNQ^{-}\cdot$ and Dewar and Rzepa[44] have carried out additional electronic structure calculations on $TCNQ^0$, $TCNQ^{-}\cdot$, and $TCNQ^{2-}$ using a MNDO-SCF-MO formalism. Since Dewar and Rzepa have reported bond lengths, r_i, calculated from MNDO results rather than bond orders, comparison with experiment will be done by computing a total, PED weighted bond length change, $\Delta R_{i,total}$, for each normal mode from

$$\Delta R_{i,total} = \sum_i (PED)_{K_i} \Delta r_i \qquad (4)$$

Thus we are now in a position to compare the experimentally determined ET induced vibrational frequency shifts for the two successive TCNQ reduction steps with the results of three different electronic structure calculations and two different potential energy distribution calculations.

Table II lists the bond-order and bond-length changes which accompany the first and second electron-transfer processes for TCNQ as determined from the theoretical electronic structure calculations.[16,42,44] These results were combined with the PEDs for $TCNQ^0$ [39] and for $TCNQ^{-}\cdot$[43] to generate the total, weighted bond-order and bond-length changes shown in Tables III and IV, respectively. The measured frequency shifts show qualitative agreement with both the sign and magnitude of the weighted bond-order and bond-length changes. Two anomalies

Table III. Weighted Bond-Order and Bond-Length Changes Based on PED of $TCNQ^0$

mode ν_i	PED (%)[a] $TCNQ^0$	$\sum_i(PED)_{K_i}\cdot\Delta p_{i,1}$[b]	$\sum_i(PED)_{K_i}\cdot\Delta p_{i,1}$[c]	$\sum_i(PED)_{K_i}\cdot\Delta r_{i,1}$,[d] pm	$\sum_i(PED)_{K_i}\cdot\Delta p_{i,2}$[b]	$\sum_i(PED)_{K_i}\cdot\Delta p_{i,2}$[c]	$\sum_i(PED)_{K_i}\cdot\Delta r_{i,2}$[d], pm
ν_1	K_1 (99)				0	0	0
ν_2	K_6 (87)	−0.044	−0.027	+0.1	−0.070	−0.028	+0.8
ν_3	K_1 (46), K_2 (22) K_3 (25), H_3 (20)	−0.063	−0.070	+1.3	−0.070	−0.061	+1.3
ν_4	K_1 (30), K_3 (59)	−0.145	−0.157	+2.9	−0.166	−0.132	+3.0
ν_5	H_3 (21)	0	0	0	0	0	0
ν_6	K_2 (45), K_4 (21)	+0.077	+0.077	−1.6	+0.095	+0.056	−1.2
ν_7	K_2 (32), K_4 (17)	+0.057	−0.056	−1.2	+0.070	+0.041	−0.9
ν_8	K_4 (23), H_6 (43) H_7 (18)	+0.021	−0.015	−0.4	+0.030	+0.012	−0.2
ν_9	H_1 (18), H_6 (18)	0	0	0	0	0	0
ν_{10}	H_6 (28), H_7 (49)	0	0	0	0	0	0

[a] From ref 39. [b] $\Delta p_{i,1}$ and $\Delta p_{i,2}$ same as in Table II; from ref 16. [c] From ref 42. [d] $\Delta r_{i,1}$ and $\Delta r_{i,2}$ same as in Table II; from ref 44.

Table IV. Weighted Bond-Order and Bond-Length Changes Based on PED of $TCNQ^-\cdot$

mode ν_i	PED (%)[a] TCNQ·	$\sum_i(PED)_{K_i}\cdot\Delta p_{i,1}$[b]	$\sum_i(PED)_{K_i}\cdot\Delta p_{i,1}$[c]	$\sum_i(PED)_{K_i}\cdot\Delta r_{i,1}$,[d] pm	$\sum_i(PED)_{K}\cdot\Delta p_{i,2}$[b]	$\sum_i(PED)_{K_i}\cdot\Delta p_{i,2}$[c]	$\sum_i(PED)_{K_i}\cdot\Delta r_{i,2}$,[d] pm
ν_1	K_6 (99)						
ν_2	K_5 (85)	−0.042	−0.0264	+0.1	−0.068	−0.272	+0.8
ν_3	K_1 (50), K_2 (25), K_3 (17)	−0.046	−0.0535	+1.0	−0.052	−0.0464	+1.0
ν_4	K_1 (23), K_3 (64)	−0.15	−0.160	+3.0	−0.17	−0.135	+3.1
ν_5	H_3 (79)	0	0	0	0	0	0
ν_6	K_2 (45), K_4 (20)	+0.076	+0.0760	−1.6	+0.094	+0.0552	−1.2
ν_7	K_2 (29), K_4 (18)	+0.054	+0.0523	−1.1	+0.067	+0.0382	−0.8
ν_8	K_4 (23), H_6 (42), H_7 (19)	+0.021	+0.0150	−0.4	+0.030	+0.0117	−0.2
ν_9	K_3 (17), H_1 (17), H_6 (18)	−0.034	−0.0360	+0.7	−0.039	−0.0309	+0.7
ν_{10}	H_6 (29), H_7 (48)	0	0	0	0	0	0

[a] From ref 43. [b] $\Delta p_{i,1}$ and $\Delta p_{i,2}$ same as in Table II; from ref. 16. [c] From ref 42. [d] $\Delta r_{i,1}$ and $\Delta r_{i,2}$ same as in Table II; from ref 44.

do, however, appear. First, the weighted bond-length change computed for ν_2 in the $TCNQ^-\cdot$ formation process is virtually zero, whereas this mode is found experimentally to show a substantial change in frequency. We attribute this anomaly to a deficiency in the MNDO calculation of the C≡N bond length change since (1) the C≡N stretch dominates the PED for the ν_2 normal mode and (2) both bond order change calculations are in agreement with the observations. Second, there is no correlation whatsoever between the ν_3 frequency shift and either the weighted bond-order or bond-length changes. The ν_3 mode frequency is observed to be almost insensitive to TCNQ oxidation state and yet there are substantial changes in the total bond-order and bond-length changes for both ET processes. The reasons for this disagreement are not completely clear at this time, but the following suggestions can be offered: (1) mode ν_3 is independent of the PED in TCNQ; (2) the electronic structure calculations fail drastically for this mode; or (3) both PEDs are markedly in error for this mode. Possibility (1) does not seem likely owing to the fact that the PED and normal modes are linked through the NCA. Possibility (2) is also difficult to rationalize since the internal coordinates involved in ν_3 are also involved in other normal modes for which the weighted bond order changes do work. Consequently, possibility (3) is regarded as the most likely explanation. That the PED is in error for this mode is given some additional credence by the fact that the NCA is only capable of reproducing the observed $TCNQ^0$ frequencies within $\pm 7.5\ cm^{-1}$ [39] and the NCA for $TCNQ^-\cdot$ gives a calculated ν_3 frequency which is 26 cm^{-1} lower than the observed value.

It should also be pointed out that the experimentally measured ET frequency shifts and their relationship to electronic structure change can also be used as an aid to the assignment of RR excitation spectra.[45] The RR excitation spectra obtained by exciting into the region of the $^2B_{3g} \rightarrow {}^2B_{1u}{}^{(1)}$ transition of $TCNQ^-\cdot$ with a tunable CW dye laser are highly structured. The energy separations between the maxima in these RR excitation spectra can be used to deduce the excited state vibrational frequencies for certain totally symmetric normal modes of $TCNQ^-\cdot{}^*$ ($^2B_{1u}$). Thus one can obtain approximate values for the vibrational frequency shifts associated with the optically excited, intramolecular electron rearrangement process:

$$TCNQ^-\cdot(^2B_{3g}) + h\nu_{laser} \rightarrow TCNQ^-\cdot{}^*(^2B_{1u}) \qquad (5)$$

The Δp_i associated with process 5 can also be obtained from certain electronic structure calculations[45] and are generally found to be smaller than the Δp_i for the corresponding one-electron intermolecular transfer. Therefore one expects that the excited-state frequencies for $TCNQ^-\cdot{}^*$ should be smaller than the corresponding frequency for $TCNQ^-\cdot$ but larger than the frequencies for $TCNQ^{2-}$. This criterion was used to restrict the search range of ν_2 in the attempt to fit the observed RR excitation spectra of $TCNQ^-\cdot$.[45]

Identification of the TCNQ Oxidation State in a Co(II) Coordination Complex. Basolo and co-workers[31] have formulated compound **3**, which is a diamagnetic, air-stable, brown solid, as the $[Co(acacen)(py)_2]^+$ salt of $TCNQ^{2-}$ rather than as the nitrile bonded dimer[46] on the basis of the elemental analysis, the electronic diffuse reflectance spectrum, and the IR spectrum in the C≡N stretching region. Such a formulation is at variance, however, with our observations of extreme O_2 reactivity for $TCNQ^{2-}$ in solution and as the solid dilithium salt. Since we now have Raman spectroscopic data for the electronic structure sensitive modes, ν_2 and ν_4, in $TCNQ^0$, $TCNQ^-\cdot$, and $TCNQ^{2-}$, we should be able to unambiguously

determine the oxidation state of the TCNQ in **3**. The Raman spectrum of **3** obtained using the 647.1-nm line of a Kr^+ laser is shown in Figure 3B. The Kr^+ laser frequency was used to minimize sample fluorescence. At this excitation wavelength one expects to obtain NRS for $TCNQ^0$ and $TCNQ^{2-}$ but RRS for $TCNQ^{-}\cdot$. The bands at 339, 610, 677, 715, 1187, 1387, 1609, 1949, and 2192 cm^{-1} are assigned to the resonance enhanced ν_9, ν_8, ν_7, ν_5, ν_3, $\nu_3 + \nu_9$, and ν_2 bands of trace quantities of $TCNQ^{-}\cdot$ formed adventitiously during the preparation and isolation of **3**. The 431- and 481-cm^{-1} lines are also found in the NRS of the Co(II) Schiff's base chelate. The 647-, 1024-, and 1048-cm^{-1} peaks are assigned to Co(II) coordinated pyridine.[47] The bands at 2164, 1492, and 1465 cm^{-1} cannot yet be confidently assigned. The remaining Raman lines at 2106, 1304, 1194, and 731 cm^{-1} can be readily attributed to the ν_2, ν_4, ν_5, and ν_7 modes of $TCNQ^{2-}$ by comparison with the NRS of $Li_2TCNQ\cdot THF$ and the RRS of electrogenerated $TCNQ^{2-}$ in CH_3CN solution. The ν_3 mode of $TCNQ^{2-}$ in **3** is probably masked by the strong, resonance enhanced ν_3 line of $TCNQ^{-}\cdot$ considering the insensitivity of this mode to electronic structure changes (see Table I). The small deviation from exact congruence between the spectral lines of $TCNQ^{2-}$ in **3** and in **1** can be rationalized in terms of cation size effects by analogy with the results of studies on the effects of cation size on the vibrational frequencies of solid $TCNQ^{-}\cdot$ salts.[40] The present Raman data on **3**, especially the clear presence of the two most electronic structure sensitive modes (ν_2 and ν_4) in Figure 3B, support Basolo's original formulation of this compound as containing $TCNQ^{2-}$. In view of the extreme O_2 sensitivity of both electrogenerated $TCNQ^{2-}$ and solid-state $Li_2TCNQ\cdot THF$, it is interesting to note that the large cation $[Co(acacen)(py)_2]^+$ is apparently able to shut off the O_2 decay reaction of $TCNQ^{2-}$ leading to the α,α-dicyano-*p*-toluoyl cyanide anion ($DCTC^-$)[17] (at least for periods of many days) as evidenced by the lack of bands corresponding to $DCTC^-$ in Figure 3B.

Conclusion

We have measured the RR spectrum of electrogenerated $TCNQ^{2-}$ and the frequency shifts which accompany its formation from the radical anion. A reasonable qualitative correlation between these shifts and the weighted bond-order and bond-length changes was obtained for all of the observed modes except ν_3. Finally this new Raman data was used to determine that the TCNQ in the coordination complex $[Co(acacen)(py)_2]_2TCNQ$ is in fact $TCNQ^{2-}$.

Acknowledgments. The authors wish to thank Professor Fred Basolo for helpful discussion, Dr. Thomas Szymanski for the preparation of the Co(acacen), and Dr. David L. Jeanmaire for his general assistance and interest in this problem. The support of this research by the National Science Foundation under Grants CHE 74-12573 A03 and CHE 75-15480 is gratefully acknowledged. In addition R.P.V.D. acknowledges support from the Alfred P. Sloan Foundation (1974-1978), M.R.S. acknowledges an Electrochemical Society Summer Fellowship (1975), J.M.L. acknowledges partial financial support from the 3M Co., and T.M.C. acknowledges an IBM Postdoctoral Fellowship.

References and Notes

(1) (a) Northwestern University. (b) Alfred P. Sloan Fellow, 1974-1978. (c) Diamond Shamrock Corp., T. R. Evans Research Center, Painesville, Ohio 44077. (d) 3M Co. (e) IBM Fellow, 1977.
(2) Efrima, S.; Bixon, M. *Chem. Phys. Lett.* **1974**, *25*, 34-37.
(3) Van Duyne, R. P.; Fischer, S. F. *Chem. Phys.* **1974**, *5*, 183-197.
(4) Fischer, S. F.; Van Duyne, R. P. *Chem. Phys.* **1977**, *26*, 9-16.
(5) Ulstrup, J.; Jortner, J. *J. Chem. Phys.* **1975**, *63*, 4358-4368.
(6) Efrima, S.; Bixon, M. *Chem. Phys.* **1976**, *13*, 447-460.
(7) Efrima, S.; Bixon, M. *J. Chem. Phys.* **1976**, *64*, 3639-3647.
(8) Garito, A. F.; Heeger, A. J. *Acc. Chem. Res.* **1974**, *7*, 232-240.
(9) Soos, Z. *Annu. Rev. Phys. Chem.* **1974**, *25*, 121-153.
(10) Goodings, E. P. *Chem. Soc. Rev.* **1976**, *5*, 95-123.
(11) Engler, E. M. *Chem. Technol.* **1976**, *6*, 274-279.
(12) Miller, J. S.; Epstein, A. J. *Ann. N.Y. Acad. Sci.* **1978**, *313*, 1-828.
(13) Jeanmaire, D. L.; Suchanski, M. R.; Van Duyne, R. P. *J. Am. Chem. Soc.* **1975**, *97*, 1699-1707.
(14) Jeanmaire, D. L.; Van Duyne, R. P. *J. Am. Chem. Soc.* **1976**, *98*, 4029-4033.
(15) The convention $\Delta\nu_i = \nu_i$(final state) $- \nu_i$(initial state) is used in this paper.
(16) Jonkman, H. T.; Kommandeur, J. *Chem. Phys. Lett.* **1972**, *15*, 496-499.
(17) Suchanski, M. R.; Van Duyne, R. P. *J. Am. Chem. Soc.* **1976**, *98*, 250-252.
(18) Tsuboi, M.; Hirakawa, A. Y.; Nishimura, Y.; Harada, I. *J. Raman Spectrosc.* **1974**, *2*, 609-661.
(19) Pezolet, M.; Yu, T.-J.; Peticolas, W. L. *J. Raman Spectrosc.* **1975**, *3*, 55-64.
(20) Ohta, N.; Ito, M. *Chem. Phys.* **1977**, *20*, 71-81.
(21) Larrabee, J. A.; Spiro, T. G.; Ferris, N. S.; Woodruff, W. H.; Maltese, W. A.; Kerr, M. S. *J. Am. Chem. Soc.* **1977**, *99*, 1979-1980.
(22) Muramatsu, S.; Naus, K.; Takahashi, M.; Kaya, K. *Chem. Phys. Lett.* **1977**, 50, 284-288.
(23) Champion, P. M.; Gunsalus, I. C. *J. Am. Chem. Soc.* **1977**, *99*, 2000-2002.
(24) Ohta, N.; Ito, M. *Chem. Phys.* **1977**, *24*, 175-181.
(25) Sugawara, Y.; Hamaguchi, H.; Harada, I.; Shimanouchi, T. *Chem. Phys. Lett.* **1977**, *52*, 323-326.
(26) Peticolas, W. L. *Proc. Int. Conf. Raman Spectrosc., 5th*, **1976**.
(27) Hong, H. K.; Jacobsen, C. W. *Chem. Phys. Lett.* **1977**, *47*, 457-461.
(28) Hong, H. K.; Jacobsen, C. W. *J. Chem. Phys.* **1978**, *68*, 1170-1184.
(29) Melby, L. R.; Harder, R. J.; Hertler, W. R.; Mahler, W.; Benson, R. E.; Mochel, W. E. *J. Am. Chem. Soc.* **1962**, 84, 3374-3387.
(30) Carter, M. J. Ph.D. Thesis, Northwestern University, Evanston, Ill., 1973, p 31.
(31) Clarkson, S. G.; Lane, B. C.; Basolo, F. *Inorg. Chem.* **1972**, *11*, 662-664.
(32) Van Duyne, R. P. *J. Phys. (Paris)* **1977**, *38*, C5-239-252.
(33) Cotton, T. M.; Van Duyne, R. P. *Biochem. Biophys. Res. Commun.* **1978**, *82*, 424-433.
(34) Cotton, T. M.; Van Duyne, R. P., manuscript in preparation.
(35) Drake, K. F.; Van Duyne, R. P.; Bond, A. M. *J. Electroanal. Chem.* **1978**, *89*, 231-246.
(36) Savitzky, A.; Golay, M. J. E. *Anal. Chem.* **1964**, *36*, 1627-1639.
(37) Tschemler, H. T.; Voettner, H. *Monatsh. Chem.* **1952**, *83*, 301-321.
(38) Jeanmaire, D. L. Unpublished results.
(39) Girlando, A.; Pecile, C. *Spectrochim. Acta, Part A* **1973**, *29*, 1859-1878.
(40) Suchanski, M. R. Ph.D. Thesis, Northwestern University, 1977, pp 118-256.
(41) Van Duyne, R. P.; Suchanski, M. R.; Cape, T. C. *J. Am. Chem. Soc.*, submitted.
(42) Krogh-Jespersen, K.; Ratner, M. A., *Theor. Chim. Acta* **1978**, *47*, 283-296.
(43) Bozio, R.; Zanon, I.; Girlando, A.; Pecile, C. *J. Chem. Soc., Faraday Trans. 2* **1978**, 235-248.
(44) Dewar, M. J. S.; Rzepa, H. S. *J. Am. Chem. Soc.* **1978**, *100*, 784-790.
(45) Jeanmaire, D. L.; Van Duyne, R. P. *J. Am. Chem. Soc.* **1976**, *98*, 4034-4039.
(46) Crumbliss, A. L.; Basolo, F. *Inorg. Chem.* **1971**, *10*, 1676-1680.
(47) Hendra, P. J.; Turner, I. D. M.; Loader, E. J.; Stacey, M. J. *J. Phys. Chem.* **1974**, *78*, 300-304.